Cognition 251 (2024) 105903

Contents lists available at ScienceDirect

Cognition

journal homepage: www.elsevier.com/locate/cognit

Viewpoint adaptation revealed potential representational differences between 2D images and 3D objects

Zhiqing Deng [a], Jie Gao [a], Toni Li [b], Yan Chen [a], BoYu Gao [c], Fang Fang [d,e,f,g], Jody C. Culham [h], Juan Chen [a,i,*]

[a] Center for the Study of Applied Psychology, Guangdong Key Laboratory of Mental Health and Cognitive Science, and the School of Psychology, South China Normal University, Guangzhou, Guangdong Province 510631, China
[b] Division of Emergency Medicine, Department of Medicine, University of Toronto, Toronto M5S 3H2, Canada
[c] College of Information Science and Technology/Cyber Security, Jinan University, Guangzhou 510632, China
[d] School of Psychological and Cognitive Sciences and Beijing Key Laboratory of Behavior and Mental Health, Peking University, Beijing 100871, China
[e] Key Laboratory of Machine Perception (Ministry of Education), Peking University, Beijing 100871, People's Republic of China
[f] Peking-Tsinghua Center for Life Sciences, Peking University, Beijing 100871, China
[g] IDG/McGovern Institute for Brain Research, Peking University, Beijing 100871, China
[h] Department of Psychology, The University of Western Ontario, London, ON N6A 5C2, Canada
[i] Key Laboratory of Brain, Cognition and Education Sciences (South China Normal University), Ministry of Education, China

ARTICLE INFO

Keywords:
3D real objects
Stereopsis
Viewpoint adaptation
Adaptation aftereffects
Tuning curve
Computational model

ABSTRACT

For convenience and experimental control, cognitive science has relied largely on images as stimuli rather than the real, tangible objects encountered in the real world. Recent evidence suggests that the cognitive processing of images may differ from real objects, especially in the processing of spatial locations and actions, thought to be mediated by the dorsal visual stream. Perceptual and semantic processing in the ventral visual stream, however, has been assumed to be largely unaffected by the realism of objects. Several studies have found that one key difference accounting for differences between real objects and images is actability; however, less research has investigated another potential difference – the three-dimensional nature of real objects as conveyed by cues like binocular disparity. To investigate the extent to which perception is affected by the realism of a stimulus, we compared viewpoint adaptation when stimuli (a face or a kettle) were 2D (flat images without binocular disparity) vs. 3D (i.e., real, tangible objects or stereoscopic images with binocular disparity). For both faces and kettles, adaptation to 3D stimuli induced stronger viewpoint aftereffects than adaptation to 2D images when the adapting orientation was rightward. A computational model suggested that the difference in aftereffects could be explained by broader viewpoint tuning for 3D compared to 2D stimuli. Overall, our finding narrowed the gap between understanding the neural processing of visual images and real-world objects by suggesting that compared to 2D images, real and simulated 3D objects evoke more broadly tuned neural representations, which may result in stronger viewpoint invariance.

1. Introduction

Cognition research has revealed much about how the brain uses vision to recognize objects, even as their visual appearance changes with viewpoint. However, this research has relied heavily on using images of objects as a convenient proxy for real objects. Unlike working with tangible 3D objects in real space, the presentation of images on a computer monitor enables fast presentation and careful experimental control of visual attributes. However, it remains unclear whether the results derived from studies of images generalize to the processing of real objects.

Compared to real objects, 2D images differ in at least two key features. First, images are intangible representations of objects that can not be acted upon. Relatedly, they do not provide information on true physical size and distance. For instance, one may see an image of a huge object, like the moon on a piece of paper within reach even though the

* Corresponding author at: Center for the Study of Applied Psychology, Guangdong Key Laboratory of Mental Health and Cognitive Science, and the School of Psychology, South China Normal University, Guangzhou, Guangdong Province 510631, China.
E-mail address: juanchen@m.scnu.edu.cn (J. Chen).

https://doi.org/10.1016/j.cognition.2024.105903
Received 9 November 2023; Received in revised form 17 July 2024; Accepted 22 July 2024

real moon would be many orders of magnitude larger and farther – and clearly unreachable. Second, images do not provide valid stereoscopic cues to depth. Indeed, stereoscopic vision of a 2D image indicates a flat surface that is inconsistent with other monocular cues to depth (e.g., shading).

Recently, researchers have reviewed how the realism of objects affects perception, action, attention, and memory (Snow & Culham, 2021). In short, people are better at recognizing real objects than matched photographs (real-object advantage) (Holler et al., 2019) and real objects may activate differences in brain activation compared to pictures (Freud et al., 2018). Real objects were not found to show repetition suppression effects widely found with images (Konen & Kastner, 2008; Snow et al., 2011). In addition, both infants and adults prefer to look at real objects (real-object preference) (Gerhard et al., 2016; Gomez et al., 2018), suggesting that real objects can capture more attention than images. Real objects are also more memorable than their 2D photographs (Snow et al., 2014). Less is known about the differences between real faces and common image proxies.

Growing evidence supports the importance of actability in accounting for differences between real objects and images (Snow & Culham, 2021). One of the strongest pieces of evidence comes from an EEG study that showed that viewing real objects triggered stronger and more sustained event-related desynchronization (ERD) in the μ frequency band (8–13 Hz) - a neural signature of automatic motor preparation (Marini et al., 2019). In the field of action, ample evidence suggests different processing for real objects compared to images. Participants were able to scale their grip aperture according to its size even when the size of the object was invisible, but this was observed only when the target object was real, not pictorial (Chen et al., 2015). Later, in an fMRI study, the neural mechanisms of grasping 2D and 3D objects were directly investigated (Freud et al., 2018). The study found that at the planning stage of grasping (i.e., before action execution), the activation of the left anterior intraparietal sulcus (aIPS), a key area for visually guided grasping actions, is affected by the realness of the grasping target.

Although actability is emerging as a key factor driving the differences between real objects and images, less is known about the degree to which visual differences – namely the presence vs. absence of stereopsis – are a factor (Burke et al., 2007). Note that actability and stereoscopic differences are not mutually exclusive. Stereopsis, in combination with realistic oculomotor cues to depth (vergence and accommodation), can be used to estimate an object's distance (and thus reachability) and infer its physical size. Stereopsis (and its consistency with monocular depth cues) is also a key fact in conveying that an object is indeed 3D and likely tangible (though not necessarily, as in virtual reality).

One notable feature of stereoscopic vision is that it simultaneously provides two views of a scene from different perspectives, providing richer information about the 3D structure of objects within the scene. For stimuli such as faces, 3D cues like stereopsis could provide richer cues regarding the volumetric form (for example, how much the nose sticks out) in addition to the information available in images (for example, how far apart the eyes are).

Some theories of object recognition postulate that information from different side views of an object is integrated to create a coherent 3D model (Biederman, 1985; Marr & Nishihara, 1978). Other theories propose that object representations can be comprised of multiple viewpoints without need for full view-invariance (Bülthoff et al., 1995) [see (Peissig & Tarr, 2007), for a review]. Neurophysiological evidence suggests a predominance of view-selective neurons within regions of the ventral visual stream (such as the superior temporal sulcus, STS, and inferotemporal cortex, IT) for both faces (De Souza et al., 2005; Desimone et al., 1984; Perrett et al., 1985; Perrett et al., 1991) and objects (Logothetis & Pauls, 1995). These neurons have bell-shaped tuning curves similar to orientation tuning curves in the primary visual cortex, V1 (Hammond & Andrews, 1978; Heggelund & Albus, 1978), or motion direction tuning curves in the middle temporal (MT) area (Kohn & Movshon, 2004).

Similar to explanations for illusions like the tilt aftereffect and motion aftereffect, after adapting to a sided-view face for a while, one would perceive a front-view face as having an orientation shifted opposite to that of the adapting view. This phenomenon has been called the face viewpoint aftereffect (Chen, Yang, et al., 2010; Fang & He, 2005). As reviewed by Webster (2011), aftereffects can be observed throughout the visual hierarchy from retina (e.g., afterimages) to early visual cortex (e.g., spatial frequency and orientation aftereffects) to mid−/high-level vision (e.g., holistic face aftereffects for attributes like gender). Consistent with the neural processing of viewpoints, face viewpoint aftereffects are thought to occur at mid/high levels of processing (Fang & He, 2005).

Neurophysiological studies of tuning curves and behavioral studies of adaptation aftereffects for faces have all used 2D face pictures as stimuli. What we see in everyday life, however, are 3D heads. The question arises then of how well results about viewpoint tuning from 2D pictures generalize to the real world. Here there are several possibilities. First, tuning curves from 2D pictures and 3D physical stimuli could be identical. Certainly, this is the assumption of the research done to date, though this assumption has not been explicitly tested, which is one goal of the present study. Tuning curves could be equivalent the case if monocular cues from flat images are sufficient to extract 3D structure. It could also be the case if adaptation is at such a high level that it is governed by the consciously perceived viewpoint, which would be more aligned with the dominant eye. Second, it could be that the two viewpoints provided when binocular disparity is present activates a broader range of viewpoint representations at relatively low levels of visual processing, leading to broader tuning curves for physical and 3D stimuli than 2D images. By this account, any presentation of multiple views would influence aftereffects, regardless of whether the two views occur simultaneously through stereopsis, over time through motion parallax, or sequentially through viewing two views side by side or alternating in time. Third, it could be that seeing an object from two viewpoints *simultaneously* through stereopsis enables extraction of a richer representation of the viewpoint at relatively late levels of visual processing, which could lead to even broader tuning than predicted by the mere availability of two viewpoints. Indeed, in one study, participants were faster and more accurate at judging whether two stimuli were the same or different (even for large viewpoint shifts) when they saw two viewpoints simultaneously through stereoscopic presentation than when they saw a single viewpoint from both eyes or two viewpoints sequentially through side-by-side viewing (Burke, 2005). Such results predict a contribution of high-level integration to object recognition. Fourth and finally, other properties beyond stereopsis could affect viewpoint tuning for physical 3D objects compared to objects presented with simulated 3D. For example, even small changes in the viewer's position can induce small amounts of motion parallax, called microparallax, which have been found to affect viewpoint perception (Wang & Troje, 2023). Alternatively, compared to 2D images or even simulated 3D, tangible physical stimuli may evoke a stronger sense of actability (Snow & Culham, 2021) and stronger recruitment of the dorsal "vision-for-action' stream (Fairchild et al., 2021; Marini et al., 2019), which could activate different neural populations with different viewpoint tuning.

To address the extent to which the 3D objects are represented differently from 2D images, we took advantage of the classic adaptation paradigm and computational modeling to probe the properties of tuning curves behaviorally and computationally (Clifford et al., 2001; Clifford & Rhodes, 2005; Seriès et al., 2004). In Experiment 1, we measured the magnitude of adaptation aftereffects as in earlier studies (Chen, Yang, et al., 2010); however, we tested not only 2D photographs but also a physical 3D face mannequin. After finding differences in this comparison, we examined what drove the difference. One possibility is the stereopsis of 3D objects. However, one experiment found that the addition of stereoscopic depth information could not explain the real-object advantage for remembering objects (Snow et al., 2023). Therefore, we then performed Experiment 2 to compare 3D stereoscopic images (with

binocular disparity) to 2D images (without binocular disparity). Previous studies suggest that stereoscopic images can evoke 3D perception and facilitate behavioral performance and brain activation and connectivity (Burke et al., 2007; Finlayson et al., 2017; Forlim et al., 2019; Gaebler et al., 2014; Snow & Culham, 2021). Moreover, evidence from other behavioral paradigms suggests that stereopsis affects viewpoint generalization (Cristino et al., 2015) and electrophysiological responses (Oliver et al., 2018).

In addition, to determine whether the possible difference in the view tuning between 3D and 2D stimuli was unique to faces, we also included an everyday object by including a real kettle, 3D stereoscopic images of the kettle, or flat 2D images of the kettle. A kettle was chosen as the stimulus because it has a similar physical size as a head and is also bilaterally symmetric. A previous study showed that although the ventral stream exhibited priming for both identical and depth-rotated images of objects, an area within the dorsal stream only exhibited priming for identical images of objects, which suggests that the dorsal stream treats rotated images as new objects (James et al., 2002). Kettles, as a kind of tool, may activate both the ventral and dorsal visual streams, and therefore, the aftereffects may be different from faces, thought to mainly activate the ventral stream. Finally, we used a computational model to simulate the adaptation effects and predict the most likely difference in the view tuning curves between 2D and 3D and between faces and kettles.

2. Experiment 1

Experiment 1 compared viewpoint adaptation aftereffects between real 3D objects and 2D images.

2.1. Materials and methods

2.1.1. Participants

Nineteen naive students (12 females and 7 males, mean age = 20) participated in Experiment 1. All participants had normal or corrected-to-normal vision, normal depth perception (tested with the Original Stereo Fly Stereotest, https://www.stereooptical.com/products/stereotests-color-tests/original-stereo-fly/. Participants all had stereoacuity of 40 arcsec or better at 16 in. viewing distance), and no history of strabismus or amblyopia. They were naive to the purpose of the experiment. They gave written informed consent. The experiment was approved by the Non-medical Research Ethics Board of the University of Western Ontario.

2.1.2. Stimuli and apparatus

Two categories of objects were used in our experiment: one face and one kettle. Both the adaptation and test stimuli were either a physical object (i.e., a face mannequin or a kettle) or a visually matched 2D pictures of the same real object. The 3D face mannequin, which was about 20 cm in height from the chin to the top of the head, roughly matched the size of an actual human head. The kettle was 19 cm in height and 23 cm width. The vertical visual angles of the mannequin and the kettle were about 6.6° and 5.4° in height, respectively.

The real objects could be manually rotated to a specific view. Within each category, the set of stimuli consisted of a frontal view (i.e., 0°) and eight side views (±3°, ±6°, ±9°, and ± 15°) ("-" denotes leftward; "+" denotes rightward from the perspective of the viewer), which were generated by projecting real-world models rotated in depth (leftward or rightward). For the face mannequin, the frontal view was defined as the view of the face-forward side. Because the mannequin was not perfectly symmetrical, the front view (i.e., 0°) of the mannequin was determined based on 13 participants' judgments during a pilot study. For the kettle, the frontal view was defined as the view in which the object appeared symmetrical and with its central components (i.e., the spout) pointing to the observer. The real objects (i.e., mannequin head or kettle) were placed on pedestal surrounded by a dial with radial scale lines to indicate the view angles to the experimenter.

For each view angle of the mannequin and the kettle, a 2D picture was taken with a Sony Alpha DSLR-A100 camera. The camera was placed at the location of the cyclopean eye (i.e., straight on, from a location that would fall between the two eyes of an actual participant). The luminance and contrast of the 2D pictures were adjusted using a MATLAB code by the experimenter and a naïve observer to match those of the real objects before the experiment.

The 2D pictures of real objects were presented on a black background via a LED screen (Dell; resolution, 1024 × 768; refresh rate, 60 Hz; Fig. 1A). The 3D real objects were placed in front of a black curtain which also provided a black background in 3D condition. Both the 2D screen and the 3D objects were placed at the back of a black board with a square opening on it. The size of the 2D images matched that of the 3D objects. The viewing distance was always 2 m. The presentation of stimuli was controlled by PsychToolbox 3 (Brainard, 1997) (http://Psychtoolbox.org/) embedded in MATLAB 2019 (MathWorks Inc., Natick MA; https://ww2.mathworks.cn/). The participants viewed the stimuli, either a single image on the monitor or a 3D real object, with both eyes.

The participants' head position was stabilized using a chin rest. A piece of privacy film switchable glass was placed in front of each participant slanted at about 45° (Fig. 1A). The switchable glass had two functions. One was to control participants' view of the stimulus (Fig. 1C, **glasses were on or off**). For example, when the experimenter was changing the viewing angle of the mannequin or kettle, the glass was opaque/off. MATLAB codes were used to control the on/off of the glass according to the timeline of the protocol. The other function was to reflect the fixation point. Specifically, to make sure that there was always a fixation point presented on the stimulus even when the glass was opaque, the fixation point was presented on the screen on the top of the whole setup and then projected to the glass. The distance between the screen and the glass was identical to the distance between the glass and the stimulus. Therefore, when participants looked at the glass, they felt like the fixation point was superimposed on the stimulus. In order to rule out the low-level (retinotopic) adaptation, the fixation point was pseudo-randomly selected from a 3 × 3 dot pattern (Fig. 1A) so that the fixation during the adaptation stage never overlapped with the fixation during the test stage. Participants would perceive the fixation point sometimes on the mannequin's eye, sometimes on the ears, or in other locations on the stimulus.

2.1.3. Design and procedure

A 2 (Dimension: 2D or 3D) × 2 (Adaptation: no adaptation or adaptation) × 2 (Category: face mannequin or kettle) × 2 (Adapting Orientation: adapt to leftward or rightward) design was adopted. The first three factors were within-subject factors whereas the last factor was a between-subject factor. Because the leftward and rightward adaptation induces aftereffects in opposite directions, we used a between-subject design for Adapting Orientation so that the leftward and rightward adaptation would not counteract each other (leftward adaptation: ten participants, rightward adaptation: nine participants).

In the 2D condition, the stimuli were 2D pictures (Fig. 1B). In the 3D condition, the stimuli were real objects. For the adaptation condition, we used a paradigm similar to the one used in a previous study (Chen, Yang, et al., 2010). An adaptation block began with a 60-s pre-adaptation period. After a 5-s top-up adaptation and a 5-s blank interval, the test stimulus was presented for 1 s. Participants were asked to make a two-alternative forced choice (2-AFC) to judge the viewing direction (leftward or rightward) of the stimulus within 5 s.

The adapting view angle was either 15° leftward or 15° rightward. Each participant only adapted to one view direction. The test stimulus could be one of seven angles (0°, ±3°, ±6°, ±9° where "-" denotes leftward; "+" denotes rightward). One difference between the current protocol and the one used in a previous study (Chen, Yang, et al., 2010) was that there were long intervals (5 s) after top-up adaptation and test

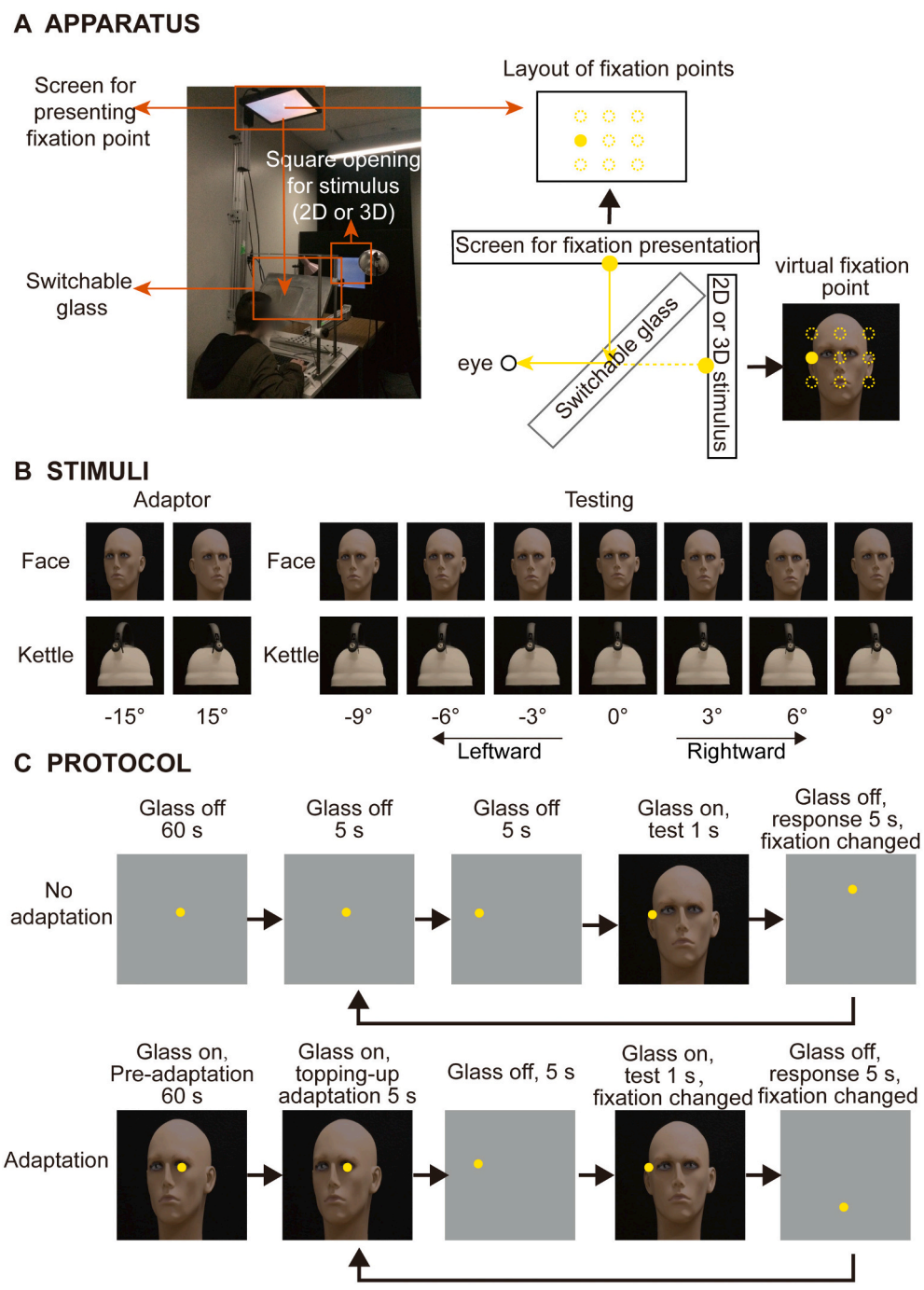

Fig. 1. Apparatus, stimuli, and protocol of Experiment 1. (**A**). In the 2D condition, a 2D image was presented on a LED screen. In the 3D condition, a real-world object (a face mannequin or a kettle) was placed on a turntable. Participants looked at the 2D images or 3D objects through a square opening on a black board. Switchable privacy glass (tilted 45° between the table plane and frontoparallel plane) was placed in front of participants' eyes to occlude their vision between adaptation/top-up and test periods and to continuously reflect fixation points on the screen above participants' head into participants' eyes. Participants perceived the fixation point at one of the 9 positions on the stimulus. In order to rule out the low-level adaptation effect, the fixation point was pseudo-randomly selected from a 3 × 3 dot pattern so that the fixation at the adaptation stage never overlapped with the fixation at the test stage (Note: the dashed dots were not presented in the experiments). (**B**). The 2D pictures were visually matched pictures of the 3D objects of a face mannequin or a kettle. Participants adapted to stimuli either rotated to the left or the right 15°. The test view could be one of the following 7 angles: 0°, ±3°, ±6° and ± 9° ("-" denotes leftward; "+" denotes rightward from the perspective of the viewer). (**C**). In the no-adaptation condition, only test stimuli were presented and participants were asked to report whether the stimulus was towards leftward or rightward. In the adaptation condition, participants adapted to the leftward or rightward face for 60-s at the beginning of the block, and then adapted another 5-s at the beginning of each trial (i.e., top-up adaptation). After a blank period of 5 s, the test stimulus was presented for 1 s. The inter-trial interval was 5 s. Note that the time course were exactly the same between the no-adaptation and adaptation conditions. The only difference between them was that no stimulus was presented at the adaptation and top-up adaptation periods in the no-adaptation condition.

stimulus to ensure that the experimenter had enough time to turn the real object to a specific angle. In addition to the adaptation block, there were also no-adaptation blocks that were used as a baseline. In the no-adaptation block, the same protocol was used except that there were no adapting objects presented at the pre-adaptation and top-up adaptation periods (Fig. 1C).

The whole study took 4 to 5 h to finish. Because of the long duration of the study, the face mannequin and kettle conditions were performed on two separate days. The order of the face mannequin and kettle conditions was randomized across participants. On each day, the experiment consisted of 8 blocks, 4 adaptation blocks, and 4 no-adaptation blocks in a random order. In each block, the adapting stimulus was kept constant, and each of the 7 test stimuli, including 0°, ±3°, ±6° and ± 9°, was presented 8 times in a random order. Each block took about 16 min. To reduce interference between adaptation and no-adaptation blocks, participants took a long break (> 5 min) between adaptation and no-adaptation blocks.

2.1.4. Data analysis

For each participant and experimental condition, we estimated the point of subjective equality (PSE), which was the angle of rotation at which the participant was equally likely to judge it as left or right (see Results for details). The viewpoint aftereffect was defined as the absolute difference between the PSE in no-adaptation condition and the PSE in the adaptation condition. A three-way ANOVA with Adapting Orientation as a between-subject factor and Dimension and Category as within-subject factors was conducted to examine the effects of Adapting orientation, Dimensions, and Category on the magnitude of viewpoint aftereffect.

Mauchly's sphericity test was used to validate ANOVAs for within-subject factors. For variables whose distribution violated sphericity, a Greenhouse–Geisser correction was performed and the results after correction were reported. Bonferroni correction was applied for multiple comparison correction. Partial eta squared (η_p^2) was calculated to indicate the effect size for ANOVAs. Values of partial eta squared of 0.0099, 0.0588, and 0.1379 are said to correspond to "small", "medium", and "large" effects, respectively (Richardson, 2011). The adjusted partial eta squared (adj η_p^2) was reported to correct the positive bias of Partial Eta Squared (Mordkoff, 2019).

All the analyses were performed with MATLAB (MathWorks Inc., Natick MA; https://ww2.mathworks.cn/) and JASP (https://jasp-stats.org/)(Love et al., 2019).

2.2. Results

2.2.1. Psychometric functions

For each participant and experimental condition, the proportion of "right" choices for each of the seven test angles generated a psychometric function. As shown in Fig. 2 (left and middle columns), psychometric functions showed the expected S-shaped curves, indicating that the proportion of "right" responses followed changes to the stimulus orientation and that the range of angles tested was appropriate to capture the full function (from 0 to 100% "right") in all conditions.

2.2.2. Point of subjective equality (PSE)

For each condition, we estimated the point of subjective equality (PSE), the angle of rotation at which the participant was equally likely to judge it as left or right.

First, we calculated the PSE in the baseline condition (i.e., no adaptation) and the adaptation condition for both the Face and the Kettle. The results from the leftward-adaptatoin group and rightward-adaptation group were collapsed. We conducted a one-sample *t*-test to

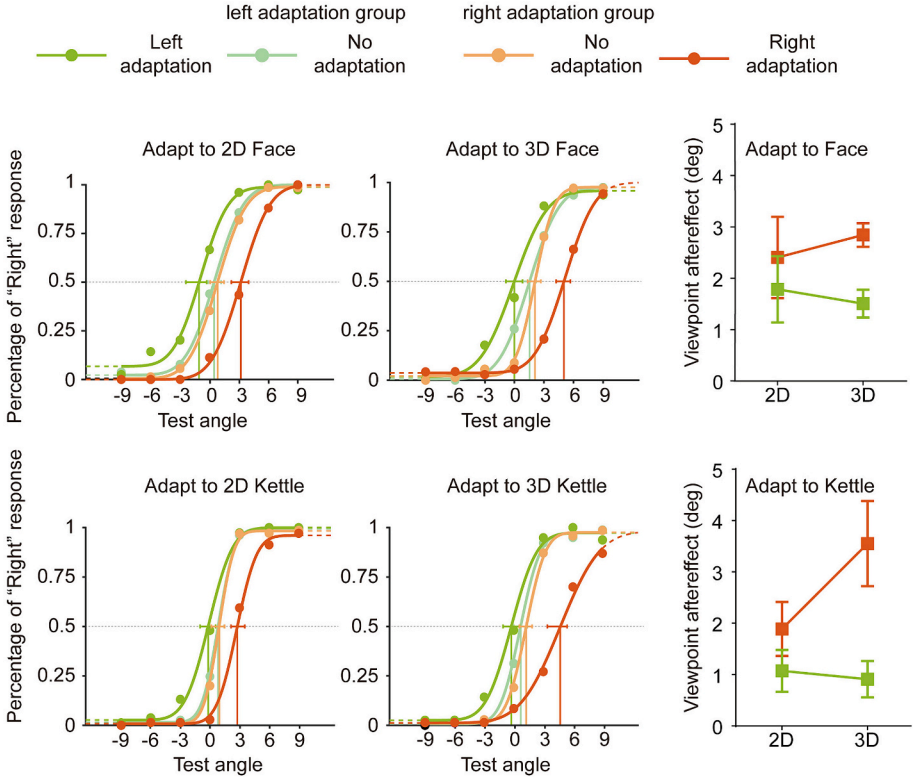

Fig. 2. Results of Experiment 1. The left and middle columns are the psychometric functions showing viewing direction judgments (i.e., percentage of trials in which participants indicated that the viewing direction was towards right) without adaptation and after adapting to 2D and 3D faces and kettles. The right column shows the magnitude of aftereffects in the left and right adaptation for 2D and 3D faces and kettles. The magnitude of aftereffects was calculated as the absolute difference between the PSE in adaptation condition and the PSE in the no-adaptation conditions. The point of subjective equality (PSE) were the test angles that correspond to 50% percept of "right" response (i.e., the intersection of the dashed horizontal line with each curve). Error bars denote ±1 SEM.

determine whether the PSE of baseline condition (i.e., no-adaptation condition) differed from 0°. We found that in all baseline conditions except the 2D face condition (2D Face: $t(18) = 2.03$, $p_{corr} = 0.057$), the PSE was significantly different from 0° (3D Face: $t(18) = 5.80$, $p_{corr} < 0.001$; 2D Kettle: $t(18) = 4.88$, $p_{corr} < 0.001$; 3D Kettle: $t(18) = 4.29$, $p_{corr} < 0.001$). In other words, participants on average did not perceive the "0°" stimulus as "front" in all conditions. This suggests that there were individual differences in view perception given that the frontal view was selected based on the pilot results of 13 participants.

2.2.3. Adaptation effects

Due to the offset and individual variance in PSE, we defined the magnitude of adaptation aftereffects as the absolute difference between PSE_{adapt} and $PSE_{no\text{-}adapt}$ separately for adaptation for each participant and each category of stimulus. As shown in Fig. 2 (right column), all adaptation aftereffects (i.e., 2D Face, 3D Face, 2D Kettle, and 3D Kettle in both left and right adaptation conditions) were statistically or marginally significant in comparisons against the null hypothesis of 0 effect (all $p_{corr} < 0.0672$).

We then compared the magnitude of aftereffects between 2D and 3D conditions. A three-way ANOVA with Adapting Orientation as a between-subject factor and Dimension and Category as within-subject factors was conducted to examine the effects of Adapting Orientation, Dimensions, and Category on the magnitude of viewpoint aftereffect.

As shown in Fig. 2 (right column), for both the face and the kettle, the viewpoint aftereffect was stronger for 3D stimuli than 2D stimuli following rightward but not leftward adaptation. This pattern was indicated by the ANOVA showing a significant interaction between Adapting Orientation and Dimension ($F(1,17) = 5.57$, $p = 0.03$, adj $\eta_p^2 = 0.203$). Simple effects analysis indicated that 3D objects produced significantly stronger aftereffects than 2D images only when adapting to the rightward viewpoint ($p_{corr} = 0.016$) but not the leftward viewpoint ($p_{corr} = 0.560$). This interaction modulated a significant main effect of Adapting Orientation ($F(1,17) = 8.29$, $p = 0.01$, adj $\eta_p^2 = 0.288$; stronger rightward adaptation than leftward adaptation) without main effects of Category ($F(1,17) = 0.45$, $p = 0.514$, adj $\eta_p^2 = -0.0324$) or Dimension ($F(1,17) = 2.38$, $p = 0.142$, adj $\eta_p^2 = 0.071$). Notably there was no interaction between Adapting Orientation and Category ($F(1,17) = 0.80$, $p = 0.385$, adj $\eta_p^2 = -0.011$), no interaction between Category and Dimension ($F(1,17) = 0.938$, $p = 0.346$, $\eta_p^2 = 0.052$, adj $\eta_p^2 = -0.004$), and no 3-way interaction ($F(1,17) = 0.638$, $p = 0.435$, adj $\eta_p^2 = -0.021$).

Overall, the pattern of results suggests stronger adaptation for physical 3D stimuli than 2D images for both faces and everyday objects. It was rather surprising that this effect was found only for rightward adaptation; notably, however, stronger aftereffects for rightward than leftward adaptation were also reported in previous studies (Chen, Yang, et al., 2010; Daar & Wilson, 2012).

3. Experiment 2

To replicate and extend the intriguing findings from the first experiment, we conducted a second experiment that utilized simulated 3D stimuli rendered through images with binocular disparity (rather than physical/tangible 3D stimuli) in comparison to 2D images.

The use of simulated 3D enabled us to test whether the effects found in Experiment 1 could be explained by the added information from binocular disparity that was available from the physical 3D stimuli. Stereoscopic 3D images also have binocular disparity, can evoke 3D perception, and can facilitate behavioral performance and brain processing (Finlayson et al., 2017; Forlim et al., 2019; Gaebler et al., 2014). Physical stimuli and images differ in many ways (see Snow & Culham, 2021 for a review). One key difference appears to be that physical stimuli can be acted upon (e.g., one could lift and rotate a physical kettle but not an image of one) (Fairchild et al., 2021; Marini et al., 2019). However, the contribution of 3D shape information from binocular vision has been less well studied. One experiment found that the addition of stereoscopic depth information could not explain the real-object advantage for remembering objects (Snow et al., 2023). However, the factors that contribute to differences between real objects and images may be dependent on the task and nature of visual processing. One plausible explanation for the results of Experiment 1 is that binocular viewing provides or invokes activation across a broader range of viewpoint-tuned channels. If so, this effect should be present for images with simulated 3D and not just tangible objects.

Our second experiment also enabled us to see whether we could replicate the surprising observation that only rightward adaptation showed a difference between 2D and 3D viewpoint adaptation. One may argue that this surprising finding was a "statistical fluke" due to the limited sample of participants in a between-subjects comparison. Moreover, the face mannequin was not perfectly symmetrical, and therefore, participants may not perceive leftward 15° and rightward 15° as comparably off-center as we expected.

Finally, the second experiment enabled us to ensure that differences between 3D and 2D stimuli were not due to low-level confounds. In Experiment 1, features like luminance and contrast were approximately matched by the experimenters. By using images for both 3D and 2D stimuli, we could ensure perfect matching.

Therefore, to replicate and extend our main finding, we performed a second experiment in which we used a within-subject design (i.e., each participant adapted to both the left and right face views but over two separate days), included a much larger sample of participants (33 participants), and adopted a different way to make 3D images, i.e., stereoscopic 3D images.

3.1. Materials and methods

3.1.1. Participants

Thirty-three naive students (19 females and 14 males, mean age = 21.8) participated in Experiment 2. All participants had normal or corrected-to-normal vision and no history of strabismus. All reported having normal stereopsis vision as revealed in their annual vision test and in the lab tested with the Original Stereo Fly Stereotest (https://www.stereooptical.com/products/stereotests-color-tests/original-stereo-fly/, participants all had stereoacuity of 40 arcsec or better at 16 in. viewing distance). They were naive to the purpose of the experiment. They gave written informed consent. The experiment was approved by the ethics committee of South China Normal University.

3.1.2. Apparatus

The stimuli were presented on a CRT monitor (ViewSonic; resolution, 1024 × 768; refresh rate, 60 Hz). The presentation of stimuli was controlled by PsychToolbox 3 (Brainard, 1997) (http://Psychtoolbox.org/) embedded in MATLAB 2019 (MathWorks Inc., Natick MA; https://ww2.mathworks.cn/). A stereoscope was used to present simulated 3D stimuli on the monitor. Notably, the use of a stereoscope rather than anaglyph glasses, provides a rich sense of stereoscopic depth without color distortions or issues of ghosting. The length of the light path from the eyes to the monitor was 60 cm for both direct viewing in the 2D condition and viewing via a mirror setup in the 3D condition (Fig. 3). The physical size and the retinal angles of the stimuli were matched. Participants' head position was stabilized using a chin rest.

3.1.3. Stimuli

Once again, two kinds of objects were used in our experiment: one face and one kettle. The stimuli subtended 2.6° of retinal angle. The size of stimuli matched a previous study (Chen, Yang, et al., 2010). These stimuli were much smaller than that used in Experiment 1 (face, 6.6° and kettle 5.4° in height) so that they could float randomly within a 6° × 6° area. Because the face and kettle were generated by software, they were perfectly symmetrical (unlike the mannequin in Experiment 1). If similar findings were observed in Experiment 2 as in Experiment 1, it would suggest that the finding could be generalized to a broad range of

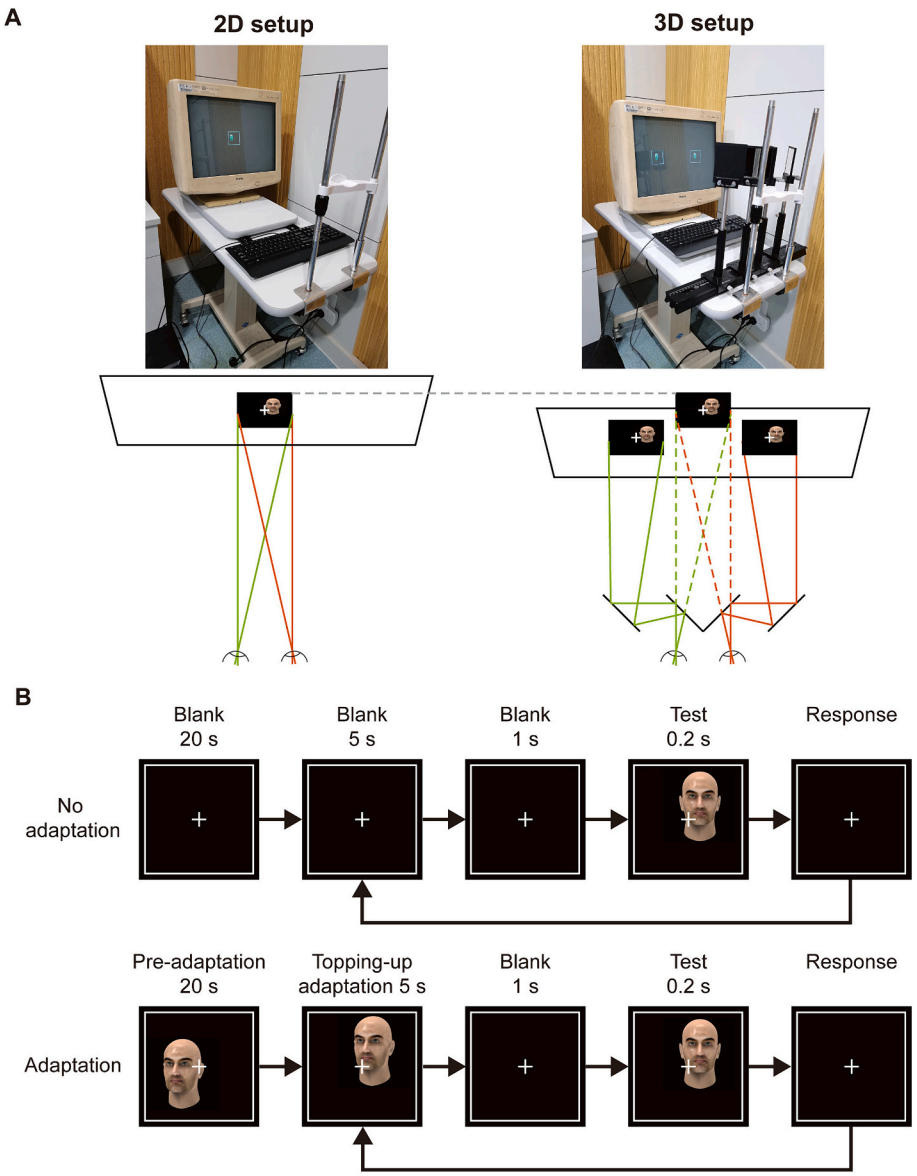

Fig. 3. Apparatus and protocol of Experiment 2. (**A**). The 2D stimuli were presented on a CRT monitor (left). In the 3D condition, two slightly different pictures were presented to each eye using a stereoscope (right). Participants perceived a single 3D object at the back of the screen (where the dashed lines pointed to). (**B**). The protocols of no-adaptation and adaptation conditions were similar to those in Experiment 1, but the adaptation stage, test stage and all blank intervals were shorter than that of Experiment 1. This was because in Experiment 2, the presentation of stimulus was controlled by the screen monitor; whereas in Experiment 1, the view angles of the real objects had to be changed manually. In addition, to rule out the possibility of low-level adaptation, the stimulus floated randomly during both adaptation and test stages within a $6° \times 6°$ area which ensured that the position of the stimulus at the adaptation stage and test stage was always different. The exact same protocol was used in this experiment as in our previous study (Chen, Yang, et al., 2010).

stimulus sizes and was not due to the asymmetry of the mannequin head.

2D images or 3D images from different viewpoints were generated from 3D models of a face and a kettle that were downloaded from TurboSquid 3D Modeling Resources (https://www.turbosquid.com/) and viewed via Autodesk 3ds Max (https://www.autodesk.com.hk/products/3ds-max) (Fig. 3A, **left**).

To generate binocular disparity for the 3D condition, two offset images were captured and presented to the respective eye. For example, a frontal view 3D image was made by presenting a $-3°$ side view image to the left eye and a $+3°$ side view to the right eye. Participants perceived a vivid sense of depth, with the object appearing to slightly protrude from the monitor surface. For the 2D condition, a single image taken from the perspective of the cyclopean eye was presented to both eyes of the participant.

3.1.4. *Design and procedure*

The design of Experiment 2 was similar to that of Experiment 1. Again, a 2 (Dimensions: 2D or 3D) $\times$ 3 (Adaptation Orientation: no adaptation, leftward adaptation or rightward adaptation) $\times$ 2 (Category: face or kettle) within-subject design was used. The only difference was that all participants performed both adapt to left and adapt to right conditions although on two separate days. In other words, Experiment 2 used a complete within-subject design.

The procedure and protocols of trials (Fig. 3B) had two additional differences from Experiment 1. First, the duration of the stimulus and intervals was shorter than those in Experiment 1 because now the presentation of stimulus was controlled by the screen monitor and there was no need to change view angles manually. Here, an adaptation block began with a 20-s pre-adaptation period. After a 5-s topping-up adaptation period and a 1-s blank interval, participants were asked to make a

2-alternative forced choice (2-AFC) to judge the viewing direction (left or right) of the stimulus. After each response, a keypress initiated the subsequent trial. The procedure of no adaptation block was similar to the adaptation block except that the pre-adaptation and topping-up adaptation had no stimulus presented into blank. Second, there was only one fixation point presented on the center of the screen. To rule out the possibility of low-level adaptation, the positions of the stimulus at the adaptation stage and test stage were always different and the adapting stimuli floated randomly within a 6° × 6° area in the velocity of 0.39°/s (Fig. 3B). The exact same protocol was used in a previous study (Chen, Yang, et al., 2010).

The experiment consisted of 24 blocks, 35 trials per block. In one block, the adapting stimulus was kept constant, and each of the seven test stimuli, including 0°, ±3°, ±6°, and ± 9°, was presented five times with a random order. Each block took about 5 min. Participants were also asked to have a rest (about 5 min) between adaptation and no-adaptation blocks so that the results in no-adaptation block were not contaminated by that in the previous adaptation block. The whole study took about 3 h, 1.5 h per day.

3.1.5. Data analysis

The aftereffects were again defined as the absolute difference in PSE between the adaptation and no-adaptation conditions. Once again, a three-way repeated measures ANOVA was conducted to examine the effect of Dimensions, Adaptation Orientation and Category on viewpoint aftereffects; however, now Adaptation Orientation was also a within-subjects variable. Mauchly's sphericity test was used to validate ANOVAs for within-subject factors. For variables whose distribution violated sphericity, Greenhouse–Geisser correction was performed and the results after correction were reported. Bonferroni correction was applied for multiple comparison correction. Adjusted partial eta squared (η_p^2) was reported to indicate the effect size for ANOVAs (Mordkoff, 2019).

3.2. Results

The results are presented in Fig. 4. We used a one-sample *t*-test to compare the PSE of baseline conditions (i.e., no adaptation condition) with 0°, and found only the PSE without adaptation in the 2D face conditions were different from 0° (2D Face: $t(32) = -2.87$, $p_{corr} = 0.029$), whereas the PSE without adaptation in the 3D face conditions and the kettle condition had no significant difference with 0 (3D Face: $t(32) = -2.30$, $p_{corr} = 0.085$; 2D kettle, $t(32) = -0.865$, $p_{corr} = 0.393$; 3D kettle, $t(32) = -1.53$ $p_{corr} = 0.272$). Because there were baseline conditions that had a PSE different from 0, we subtracted the baseline PSE from the PSE in the adaptation condition to obtain the magnitude of aftereffects.

The aftereffects, defined as the absolute value of PSE_{adapt}-$PSE_{no\text{-}adapt}$, were significantly different from 0 in all adaptation conditions (i.e., 2D Face, 3D Face, 2D Kettle, and 3 Kettle in both leftward and rightward adaptation conditions, all $p_{corr} < 0.001$).

We then used a three-way repeated ANOVA to analyze the effects of Adapting Orientations, Dimension and Categories on aftereffects. As shown in Fig. 4 (right column), the results of Experiment 2 effectively replicated the patterns seen in Experiment 1. Once again, viewpoint adaptation was stronger for 3D stimuli than 2D stimuli, but only for rightward adaptation. Specifically, once again, the interaction between Adapting Orientation and Dimension was significant ($F(1,32) = 4.94$, $p = 0.034$, adj $\eta_p^2 = 0.107$). Further analysis showed that the 3D condition produced significantly stronger aftereffects than the 2D condition but only after adapting to the rightward stimuli ($p_{corr} < 0.001$), which is consistent with our main finding in Experiment 1.

The main effect of Dimension ($F(1,32) = 16.32$, $p < 0.001$, adj $\eta_p^2 = 0.317$) and Category ($F(1,32) = 43.25$, $p < 0.001$, adj $\eta_p^2 = 0.562$) were significant which manifested as a strong aftereffect for 3D than for 2D and for faces than for kettles. The main effect of Adapting Orientations was not significant ($F(1,32) = 1.355$, $p = 0.253$, adj $\eta_p^2 = 0.011$), nor

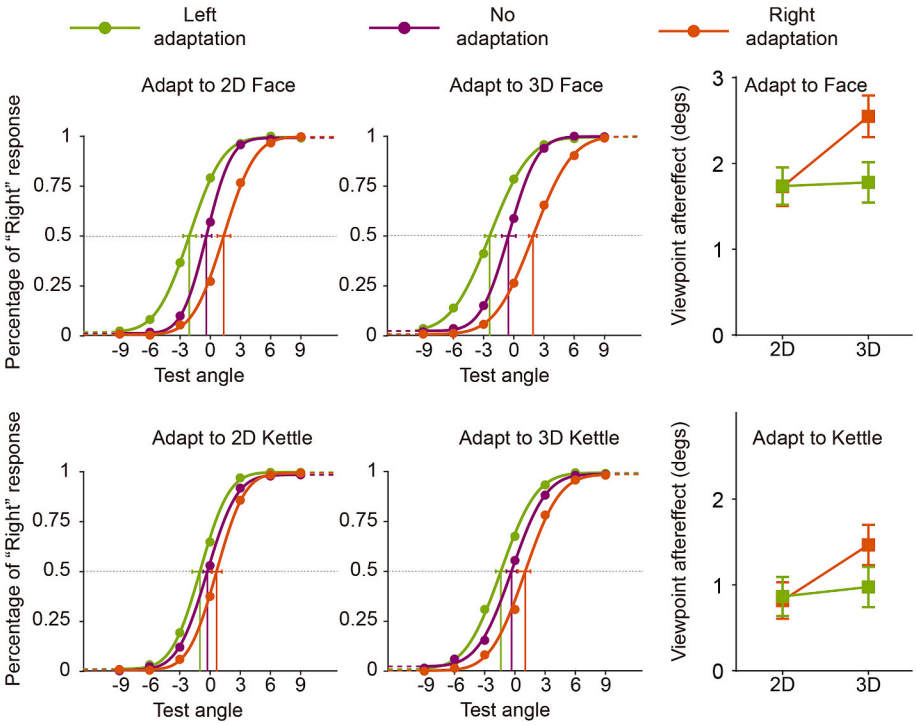

Fig. 4. Results of Experiment 2. The left and middle columns are the psychometric functions showing viewing direction judgments (i.e., percentage of trials in which participants indicated that the viewing direction was towards right) without adaptation and after adapting to 2D and 3D faces and kettles. The right column shows the magnitude of aftereffects in the left and right adaptation for 2D and 3D faces and kettles. The magnitude of aftereffects was calculated as the absolute difference between the PSE in adaptation condition and the PSE in the no-adaptation conditions. The point of subjective equality (PSE) were the test angles that correspond to 50% percept of "right" response (i.e., the intersection of the dashed horizontal line with each curve). Error bars denote 1 SEM.

were the two-way interactions between Adapting Orientation × Category, Category × Dimension and the three-way interaction of Adapting Orientation × Category × Dimension (all $p > 0.616$).

4. Computational modeling

So far, we used either 3D real objects or 3D stereoscopic images as stimuli to investigate whether the adaptation aftereffect would be different for 3D objects and 2D images. We found that only when participants adapted to the rightwards objects were the aftereffects for 3D objects significantly larger than for 2D images. We conducted a computational model to examine why the aftereffect was stronger for 3D than 2D for rightward adaptation.

Based on electrophysiological data, neurons in the temporal cortex of monkeys respond selectively to face views (Perrett et al., 1985; Perrett et al., 1991; Perrett et al., 1992). Most neurons have bell-shaped tuning function to face views with peak responses at the preferred view, and smaller responses as the view deviates from the preferred view, similar to the tuning function of V1 neurons to orientation (Hammond & Andrews, 1978; Heggelund & Albus, 1978). Here we tested specifically whether or not the tuning curves in the temporal cortex are different for 3D and 2D which results in the stronger aftereffect for 3D adaptation than 2D adaptation.

To simulate the tuning curves, the adaptation effects, and the readout of the perceived viewpoint, we designed a computational model following Clifford et al. (2001) and a previous study (Chen, Yang, et al., 2010). In the model, we assume that the tuning curves are evenly distributed before adaptation and the tuning curve of each neuron was simulated with a circular normal distribution function as below:

$$\mathbf{f}(\boldsymbol{\theta}) = \boldsymbol{\alpha} exp\{\boldsymbol{\beta}[cos(\boldsymbol{\theta} - \boldsymbol{\theta_0}) - \mathbf{1}]\}$$

where α is the peak response, β controls the bandwidth, and θ_0 is the preferred view (Fig. 5A). θ_0 is evenly distributed with a *step* of 10°. Therefore, the parameters that can determine the tuning curves include the *Step* which reflects the density of the distribution of tuning curve, the peak response (α), the bandwidth (β), and the preferred view (θ_0).

Previous studies show that the effects of adaptation on neural tuning functions mainly manifest in three ways, the suppression of peak response, the change of bandwidth, and the shift of preferred orientation (Dragoi et al., 2000; Grill-Spector et al., 2006; Kohn & Movshon, 2004; Krekelberg et al., 2006). Here, for simplicity, we assumed the effect of adaptation was constant for 2D and 3D and only tested what kind of properties of the tuning curves themselves before adaptation would induce a larger aftereffect.

Three formulae were used to simulate the changes in α, β, and θ_0 (seeChen, Yang, et al., 2010 for details) caused by adaptation (i.e., the suppression of peak response, the change of bandwidth, and the shift of preferred orientation). The parameters that best fit the results in (Chen, Yang, et al., 2010) were used to simulate the adaptation effect for both 2D and 3D. The perceived view was read out as the vector sum of a population of neurons had a bell-shaped tuning function to object view (Fig. 5) (Averbeck et al., 2006).

First, because the 2D images were photographs of 3D objects and participants perceived them as the same view, there is no reason that the preferred view varies with the dimension of the stimuli before adaptation. Therefore, we assumed that θ_0 was constant for 2D images and 3D objects.

Next, we tested the effects of the density of the distribution of tuning curves (Step, i.e., the density of the distribution of the preferred view angles), the peak response, and the bandwidth of tuning curves on the magnitude of aftereffect. We found that when the peak response ($\alpha = 1$) and the preferred view were fixed, and a moderate of bandwidth was selected ($\beta = 3.5$), changes in density of tuning curves (Step) would not significantly affect the aftereffects as long as the two tuning curves were not separated larger than about 20° (Fig. 6A). When the preferred views of the tuning curves were separated larger than 30°, the magnitude of aftereffects gets smaller with the increase of steps. However, according to previous electrical physiological studies (Perrett et al., 1991) the distribution of tuning curves for face view is much denser than 20° especially around the characteristic views (i.e., front (0°), left profile, right profile and back of head) and for right view angles. Therefore, it is unlikely that 3D stimuli changed the density of the distribution of tuning curves during rightward adaptation.

Previous fMRI results found that the overall response strength was not different between 2D images and 3D real objects in the temporal cortex (Snow et al., 2011). We also found that when the other three parameters were constant, changes in peak response (i.e., α from 0 to 1)

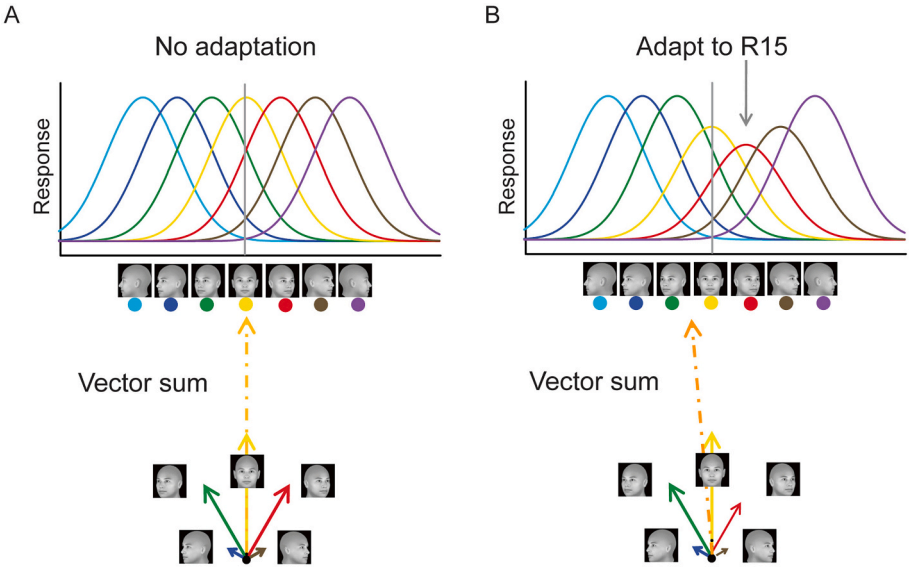

Fig. 5. Schematic diagram of population coding and vector summation before and after adaptation. (**A**) In the no-adaptation condition, the tuning curves preferred left viewpoints and right viewpoints were symmetrical, and therefore, people perceived the frontal viewpoint as front. (**B**) When people adapted to the Right 15° (R15), the response of the neurons that prefer Right 15° and close to Right 15° were suppressed, and the bandwidth and preferred viewpoint of the tuning curves may also change which resulted in a left bias (i.e., aftereffect) of the frontal viewpoint. The faces in the diagram were generated by projecting a 3D face model (FaceGen Modeller 3.1, http://www.facegen.com/) with variant in-depth rotation angles onto the monitor plane.

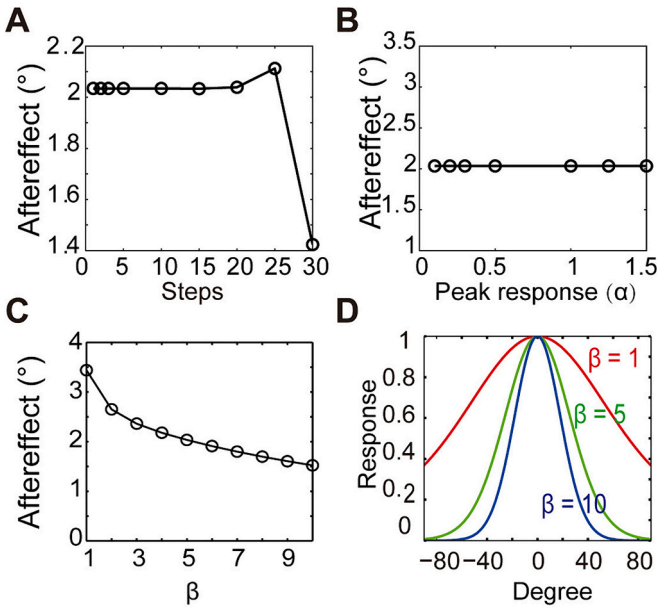

Fig. 6. Simulation results of the model. (**A**) The magnitude of aftereffects when the density of tuning curves (step) were manipulated. The horizontal axis shows the separation between two nearby tuning curves. (**B**) The magnitude of aftereffects when the peak response of tuning curves were manipulated. (**C**) The magnitude of aftereffects when the beta value that controls the width of the tuning curves was manipulated. (**D**) A larger beta value corresponds to a smaller bandwidth.

would not change the magnitude of aftereffects (Fig. 6B), and therefore, the possibility of the difference in peak response between 2D and 3D was also excluded.

Lastly, we manipulated the bandwidth of the tuning curves (i.e., beta) but kept the other parameters constant (i.e., $\alpha = 1$, Step = 10°). Results showed that with the beta values (arbitrary unit) increased from 1 (giving a full-width at half-height of 72°) to 10 (giving a full-width at half-height of 21°), the aftereffects decreased from 3° to 1.5° (Fig. 6C and D) which is within the range of aftereffects we observed in Experiments 1 and 2. In other words, the smaller the beta value, the broader the tuning curve, and as a result, the larger the adaptation aftereffect.

All in all, based on the analysis and simulation above, we suggest any differences in adaptation aftereffects between 2D and 3D would likely arise from the difference in the bandwidth of tuning curves between 2D and 3D which supports that the tuning curves for 3D may be broader than that for 2D. Note that the model does not discern the cause of broader tuning curves for 2D vs. 3D stimuli, which could arise from either low-level explanations (because a broader range of views is seen with the two eyes) or high-level explanations (because 3D provides a richer volumetric representation of the stimulus).

It should be noted that our model above was designed to simulate the stronger aftereffect for 3D than 2D in the rightward adaptation. For simplicity, symmetrical and evenly distributed tuning curves were assumed. As a result, the above model could not be used to explain the null difference between 3D and 2D in the leftward adaptation.

Although without statistical analysis, Perrett and colleagues (Perrett et al., 1991) did show a trend of asymmetry in the distribution of the preferred view angles (see their Fig. 10). Specifically, more cells show a preference for the angles within 22.5° of putative characteristic view (i.e., front, left profile, right profile, and backward views), and more importantly, more cells show a preference for right views and the distribution of preferred view angles is denser for right views than for left views. Is it possible that the null difference between 3D and 2D in leftward adaptation was due to the sparse distribution of left view angles, which made the broadening of tuning curves caused by 3D objects

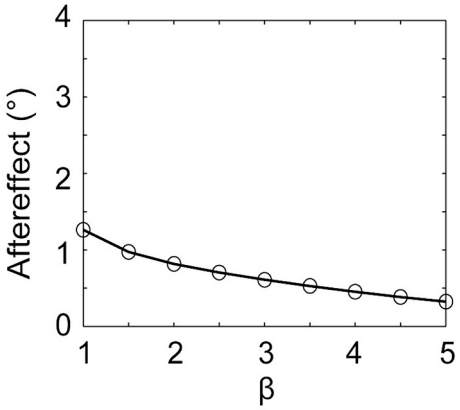

Fig. 7. Simulation results of the effect of bandwidth on the magnitude of aftereffect when the model has a large Step value (60°) between tuning curves.

ineffective in modulating the magnitude of aftereffects?

To test this, we manipulated the bandwidth of the tuning curves (i.e., β from 1 to 5) with a large Step value (= 60°) but kept the other parameters constant ($\alpha = 1$) to demonstrate the effect of sparse distribution of preferred view angles on the implementation of the broadening of tuning curves. As shown in Fig. 7, for the sparse distribution of tuning curves, the change of beta values only slightly affects the magnitude of aftereffects. Therefore, we suggest that the null-difference between 3D and 2D in leftward adaptation could be due to a sparser distribution of tuning curves for left angles.

In sum, these model demonstrates that the most likely mechanism to explain differences in the viewpoint aftereffects between 2D and 3D stimuli is differences in the viewpoint tuning bandwidth rather than in other factors like changes in peak response or shifts in the preferred orientation. The model provides explicit, testable predictions for future neurophysiological and brain imaging studies of viewpoint tuning. Specifically, the model predicts wider tuning functions for 3D stimuli and, based on our data here, perhaps also differences in the bandwidth for leftward and rightward orientations.

5. Discussion

We found that 3D faces and objects evoked stronger viewpoint aftereffects than 2D images, albeit only after rightward adaptation (a result that was replicated across two stimuli and two experiments). Importantly, viewpoint aftereffects (following rightward adaptation) were stronger for 3D stimuli than 2D stimuli regardless of whether the 3D stimuli were tangible objects or stereoscopic images, suggesting that binocular information from the two eyes was the critical factor in the difference. The computational model simulation suggested that the tuning curve of neurons for 3D stimuli may be broader than that for 2D stimuli, providing a testable prediction for future studies.

In the Introduction, we postulated four possible outcomes – (1) no difference in viewpoint aftereffects between 2D images and physical or 3D stimuli, (2) a difference between 2D stimuli and 3D stimuli (whether physical or simulated 3D stimuli) due to the availability of multiple views (whether simultaneous or not); (3) a difference between 2D and 3D stimuli due to the *simultaneously* availability of multiple views via stereopsis; and (4) a difference between 2D stimuli an 3D physical stimuli that goes above and beyond differences in stereopsis. Our results do indeed show a difference, ruling out the first possibility, and show that the effect occurs for both physical objects and simulated 3D objects, ruling out the fourth possibility. Our results suggest that 2D and 3D stimuli differ, regardless of whether the 3D is derived from physical objects or 3D simulations.

Why is the tuning curve for 3D stimuli broader than that for 2D images? One possible explanation, of course, is that viewing a stimulus

from the simultaneous perspectives of the two eyes does indeed provide a broader range of viewpoints, though the viewpoint difference is rather small, and thus stimulates a broader range of viewpoint-selective tuning curves. For example, for the physical 3D stimuli in Experiment 1, the two eyes (separated by the typical interpupillary distance of ~6.5 cm at a viewing distance of 2 m) would provide two viewpoints separated by about ±1° such that the adapting stimulus presented at 15° rotation would appear to be rotated by 14° and 16° by the two eyes. In Experiment 2, these differences were exaggerated to ±3°, though notably, this did not dramatically change the magnitude of the aftereffects, as would be predicted by this explanation.

Although the viewpoint difference between two eyes (i.e., the low-level explanation) may seem rather trivial, it nevertheless highlights the fact that the reliance on images for the study of viewpoint neglects the fact that in the real-world objects are seen from two viewpoints, even though laboratory experiments provide only a single cyclopean image. This low-level explanation brings up interesting questions about the contribution of eye dominance to such effects: Although the retinas receive two different images, the image from the dominant eye can have a stronger influence on the viewpoint perceived. That is, although two viewpoints reach the retina, only one may be perceived. Alternatively, the degree to which one eye predominates appears to depend upon the quality of individuals' depth perception, with greater fusion in individuals with good stereopsis (Wang et al., 2021; Weinman & Cooke, 1982).

Alternatively, there is also a more intriguing high-level explanation for the differences between the 2D and 3D adaptation aftereffects: Perhaps seeing a stimulus *simultaneously* from two different viewpoints through binocular disparity evokes a broader representation of viewpoint beyond the actual viewpoints seen by the two eyes. Indeed, Burke (2005) found that only with a stereoscope, the effects of viewpoint differences (viewpoint costs) were smaller than those in the synoptic presentation condition (i.e., the same view of an object in each eye), which suggests that the contribution of 3D vision to object recognition goes above and beyond the low-level availability of two different perspectives, requiring instead high-level integration through stereopsis. Consistent with this, face perception was found to be dependent upon the depth relationship between a face and an occluder (which could be reversed by swapping the views seen by the two eyes pseudoscopically), suggesting a role of high-level representation of 3D face processing (Chen, Zhou, et al., 2010) Future experiments on viewpoint adaptation could further disentangle low-level vs. high-level explanations by presenting the two eyes' views simultaneously (to evoke disparity and stereopsis), in a smooth sequence via motion parallax, or abruptly with side-by-side or temporally alternating views. Moreover, experiments could compare performance for the natural 3D structure (left/right eye view to the left/right eye, respectively) vs. reversed or "pseudoscopic" structure (left/right view to the right/left eye) (Palmisano et al., 2016). By the low-level account, any situation that provided two different views would lead to broader tuning; whereas, by a high-level account, only the situations that provided ecologically valid 3D structure (natural 3D through stereopsis and perhaps motion parallax) would be integrated to lead to broader viewpoint tuning.

Our finding of broader viewpoint tuning for 3D than 2D stimuli is consistent with other recent findings. Specifically, participants were better at recognizing volumetric objects from familiar and unfamiliar viewpoints when they learned them with vs. without stereopsis (Bennett & Vuong, 2006; Cristino et al., 2015; Oliver et al., 2018). Moreover, stereoscopic and monocular displays evoked differences in the amplitude of brain responses, as measured by event-related potentials (Oliver et al., 2018). Evidence also suggests that object recognition is enhanced when participants see a range of viewpoints by actively walking around objects (Simons et al., 2002) or by actively manipulating the object (Harman et al., 1999). Importantly, prior studies all utilized an object recognition task and investigated how recognition generalizes across viewpoints, whereas, our study examines a different task, viewpoint aftereffects. Nevertheless, the general conclusions from the two tasks agree: Seeing an object from the simultaneous perspective of the two eyes evokes a broader representation of viewpoint than that from a single eye. This interpretation could be further tested with approaches like multivoxel pattern analysis in functional magnetic resonance imaging.

Our finding that 3D stimuli evoke broader viewpoint representations than 2D stimuli can inform models of object recognition. Theories of object recognition differ in whether they postulate viewpoint invariance at later processing stages (e.g., (Biederman, 1987; Marr & Nishihara, 1978) or not (e.g., (Tarr & Bülthoff, 1998)). As argued by Burke (2005), at minimum, the effects of stereopsis on viewpoint generalization – and here viewpoint aftereffects – suggest that even if visual processing does not reach full viewpoint invariance, the representations of specific viewpoints contain some 3D information. Specifically, 3D cues provide added information about surface curvature, slant, and the spatial relationships between object parts. Moreover, 3D images evoke enhanced fMRI activation compared to 2D images not only in dorsal-stream regions implicated in visually guided actions but also in ventral-stream regions implicated in object recognition (e.g., (Durand et al., 2007; Durand et al., 2009; Janssen et al., 2018; Verhoef et al., 2016). Our findings also suggest that deep neural networks may be better able to model the human (and primate) visual system better if trained on double (stereoscopic) vs. single (monocular) views.

Previous studies on the perception of objects and faces from individual depth cues, such as surface, texture, structure from motion, and stereopsis, have highlighted the depth-cue invariant representations of objects with adaptation aftereffects (Akhavein et al., 2018; Akhavein & Farivar, 2017; Dehmoobadsharifabadi & Farivar, 2016). In our experiments, the low-level features, including luminance, contrast, and size, were matched between 2D and 3D stimuli. Nevertheless, we still observed differences in the magnitude of aftereffects, which revealed a degree of specificity for 2D information and 3D information with stereopsis.

We observed smaller aftereffects for kettles than for faces in both experiments. A previous study showed that although the ventral stream exhibited priming for both identical and depth-rotated images of objects, a dorsal-stream area only exhibited priming for identical images of objects, which suggests that the dorsal stream treated rotated images as new objects (James et al., 2002). In other words, the dorsal stream appears more sensitive to object views, suggestive of narrower tuning curves. If this were the case, according to the simulation above that narrower tuning curves resulted in smaller aftereffects (Fig. 6C and D), one would predict smaller aftereffects for kettles than for faces, which is the same outcome as we observed in Experiments 1 and 2 and suggests that our computational model can effectively predict and simulate the neural mechanisms for viewpoint adaptation regardless of object categories.

It was surprising to find stronger viewpoint aftereffects for 3D vs. 2D adaptation only after rightward but not leftward adaptation. Nevertheless, the same result was observed four times, across two stimulus categories and two experiments with different methodologies, making it unlikely to be a statistical fluke or an artifact. Moreover, the result is corroborated by a previous study (Chen, Yang, et al., 2010) and other studies (Daar & Wilson, 2012) that found larger aftereffects after rightward adaptation than leftward adaptation. Asymmetries are well known in the processing of faces. For example, when a front-facing face is viewed, the side of the face in the viewer's left visual field (i.e., the right side of the person portrayed) has a stronger effect on perception than the opposite side, perhaps because this is the side that projects predominantly to the viewer's right hemisphere, where the lateralized face-selective areas show stronger responses (Calder et al., 2008; Harrison & Strother, 2018; Yovel et al., 2008). This result seems rather at odds with the findings from portraiture that the person portrayed is often facing towards the viewer's left, such that more of the left side of their face, thought to be more influenced by emotional processing

lateralized to the right hemisphere (Nicholls et al., 1999).

Based on known asymmetries, asymmetric viewpoint adaptation for faces may be explainable. However, we also found a comparable asymmetry for an everyday object – a kettle – for which asymmetries and lateralization are not thought to be strong. Therefore, the viewpoint adaptation asymmetry is not specific to an object category but a generalized property for viewpoint representation. Unfortunately, a systematic and quantitative analysis of viewpoint tuning of cells selectively responsive to a specific view is lacking for everyday objects, although a study by (Perrett et al., 1991) does show a trend of asymmetry in the distribution of the preferred view angles. Specifically, more cells show a preference for the angles within 22.5°of putative characteristic view (i.e., front, left profile, right profile, and backward views), and more importantly, more cells show a right preference close to frontal views (see their Fig. 10). In other words, the tuning curves are more densely distributed around for right viewpoint. Our modeling results suggest that a sparse tuning could make the broadening of the tuning curve on aftereffects ineffective in magnifying the aftereffects, which may explain why no 3D and 2D difference in aftereffects was observed for leftward adaptation.

One limitation of our study is that we only tested two objects (a face and a kettle) and two adapted viewpoints (+15° and − 15°). Due to the long duration of testing sessions, such limitations are inherent in aftereffect studies (e.g., (Fang & He, 2005)). Nevertheless, results were consistent across the two experiments despite the use of different face and kettle exemplars (and despite the two face stimuli being quite different), providing corroborating evidence. Notably our experiments used relatively large samples of naïve participants ($n = 19$ and $n = 33$ in Experiments 1 and 2), unlike many psychophysical experiments which may only test 3–4 participants but across more conditions (e.g., (Fang & He, 2005) show data from $n = 4$). While this limits the amount of data per participant, it ensures that results are likely to generalize to the broader population. Another limitation common to psychophysical adaptation approaches is that the long testing sessions require repeated exposure to the same stimuli which could affect neural representations. Future studies can explore whether the same findings work for other objects and whether there were differences between 3D adaptation and 2D adaptation in other aspects, such as the transfer across face identity, gender, or even across object categories. Such studies would benefit from prior "titration" to determine whether adaptation effects can be induced with briefer adaptation and top-up periods and thus shorter testing sessions. Alternatives to psychophysics, including neurophysiology, fMRI adaptation (Grill-Spector & Malach, 2001) or representational similarity analysis in fMRI (Kriegeskorte et al., 2008) could enable relatively rapid assessment of viewpoint tuning – and its dependence upon 2D vs. 3D stimuli – across a variety of stimuli.

6. Conclusion

Overall, our study showed a compelling behavioral difference in suggesting that our understanding of viewpoint processing and viewpoint tuning functions depends upon whether or not stimuli are viewed from the simultaneous perspectives of the two eyes through stereopsis, as is typical in the real world. Past research examining differences in the way that real objects and image proxies are processed in the brain has suggested that actability is one key factor. Our results here show that the 3D depth information provided by stereopsis can also be a crucial factor. Thus, a move towards using richer stimuli – real objects and virtual simulations – may be important for understanding visual function in the real world. By narrowing the gap between understanding the neural processing of visual images and real-world objects, our results have important implications for the design of deep neural networks that will be able to work in real environments interacting with real objects.

CRediT authorship contribution statement

Zhiqing Deng: Writing – original draft, Formal analysis, Data curation. **Jie Gao:** Methodology, Data curation. **Toni Li:** Data curation. **BoYu Gao:** Methodology. **Fang Fang:** Writing – review & editing, Conceptualization. **Jody C. Culham:** Writing – review & editing, Supervision, Funding acquisition. **Juan Chen:** Conceptualization, Supervision, Project administration, Methodology, Data curation, Writing - original draft, Writing - review & editing, Funding acquisition.

Declaration of competing interest

The authors declare no competing financial interests.

Data availability

The data are available at https://osf.io/8apbw/.

Acknowledgments

This research was supported by the National Science and Technology Innovation 2030 Major Program (STI2030-Major Projects 2022ZD0204802 to JC and FF) and two National Natural Science Foundation of China (No. 31970981 and No. 31800908 to JC) . We thank Adel Al-Qawasmi for assisting with collection of pilot data, Kevin M. Stubbs for help with creating the stimuli of Experiment 1, and Derek Quinlan for technique support in experiment 1. We also thank Xiaojie Art Studio for help with generating the 3D models and 2D images in Experiment 2.

References

Akhavein, H., Dehmoobadsharifabadi, A., & Farivar, R. (2018). Magnetoencephalography adaptation reveals depth-cue-invariant object representations in the visual cortex. *Journal of Vision, 18*(12), 6. https://doi.org/10.1167/18.12.6

Akhavein, H., & Farivar, R. (2017). Gaze behavior during 3-D face identification is depth cue invariant. *Journal of Vision, 17*(2), 9. https://doi.org/10.1167/17.2.9

Averbeck, B. B., Latham, P. E., & Pouget, A. (2006). Neural correlations, population coding and computation. *Nature Reviews Neuroscience, 7*(5), 358–366.

Bennett, D. J., & Vuong, Q. C. (2006). A stereo advantage in generalizing over changes in viewpoint on object recognition tasks. *Perception & Psychophysics, 68*(7), 1082–1093.

Biederman, I. (1985). Human image understanding: Recent research and a theory. *Computer Vision, Graphics, and Image Processing, 32*(1), 29–73.

Biederman, I. (1987). Recognition-by-components: A theory of human image understanding. *Psychological Review, 94*(2), 115.

Brainard, D. H. (1997). The psychophysics toolbox. *Spatial Vision, 10*(4), 433–436. https://doi.org/10.1163/156856897x00357

Bülthoff, H. H., Edelman, S. Y., & Tarr, M. J. (1995). How are three-dimensional objects represented in the brain? *Cerebral Cortex, 5*(3), 247–260.

Burke, D. (2005). Combining disparate views of objects: Viewpoint costs are reduced by stereopsis. *Visual Cognition, 12*(5), 705–719.

Burke, D., Taubert, J., & Higman, T. (2007). Are face representations viewpoint dependent? A stereo advantage for generalising across different views of faces. *Vision Research, 47*(16), 2164–2169. https://doi.org/10.1016/j.visres.2007.04.018

Calder, A. J., Jenkins, R., Cassel, A., & Clifford, C. W. (2008). Visual representation of eye gaze is coded by a nonopponent multichannel system. *Journal of Experimental Psychology: General, 137*(2), 244.

Chen, J., Sperandio, I., & Goodale, M. A. (2015). Differences in the effects of crowding on size perception and grip scaling in densely cluttered 3-D scenes. *Psychological Science, 26*(1), 58–69. https://doi.org/10.1177/0956797614556776

Chen, J., Yang, H., Wang, A., & Fang, F. (2010). Perceptual consequences of face viewpoint adaptation: Face viewpoint aftereffect, changes of differential sensitivity to face view, and their relationship. *Journal of Vision, 10*(3). https://doi.org/10.1167/10.3.12

Chen, J., Zhou, T., Yang, H., & Fang, F. (2010). Cortical dynamics underlying face completion in human visual system. *The Journal of Neuroscience, 30*(49), 16692–16698. https://doi.org/10.1523/jneurosci.3578-10.2010

Clifford, C. W. G., & Rhodes, G. (2005). *Fitting the Mind to the World: Adaptation and After-Effects in High-Level Vision*. Oxford University Press.

Clifford, C. W. G., Wyatt, A. M., Arnold, D. H., Smith, S. T., & Wenderoth, P. (2001). Orthogonal adaptation improves orientation discrimination. *Vision Research, 41*(2), 151–159. https://doi.org/10.1016/S0042-6989(00)00248-0

Cristino, F., Davitt, L., Hayward, W. G., & Leek, E. C. (2015). Stereo disparity facilitates view generalization during shape recognition for solid multipart objects. *The Quarterly Journal of Experimental Psychology, 68*(12), 2419–2436.

Daar, M., & Wilson, H. R. (2012). The face viewpoint aftereffect: Adapting to full faces, head outlines, and features. *Vision Research, 53*(1), 54–59.
De Souza, W. C., Eifuku, S., Tamura, R., Nishijo, H., & Ono, T. (2005). Differential characteristics of face neuron responses within the anterior superior temporal sulcus of macaques. *Journal of Neurophysiology, 94*(2), 1252–1266.
Dehmoobadsharifabadi, A., & Farivar, R. (2016). Are face representations depth cue invariant? *Journal of Vision, 16*(8), 6. https://doi.org/10.1167/16.8.6
Desimone, R., Albright, T. D., Gross, C. G., & Bruce, C. (1984). Stimulus-selective properties of inferior temporal neurons in the macaque. *Journal of Neuroscience, 4*(8), 2051–2062.
Dragoi, V., Sharma, J., & Sur, M. (2000). Adaptation-induced plasticity of orientation tuning in adult visual cortex. *Neuron, 28*(1), 287–298.
Durand, J.-B., Nelissen, K., Joly, O., Wardak, C., Todd, J. T., Norman, J. F., … Orban, G. A. (2007). Anterior regions of monkey parietal cortex process visual 3D shape. *Neuron, 55*(3), 493–505.
Durand, J.-B., Peeters, R., Norman, J. F., Todd, J. T., & Orban, G. A. (2009). Parietal regions processing visual 3D shape extracted from disparity. *NeuroImage, 46*(4), 1114–1126.
Fairchild, G. T., Marini, F., & Snow, J. C. (2021). Graspability modulates the stronger neural signature of motor preparation for real objects vs. pictures. *Journal of Cognitive Neuroscience, 33*(12), 2477–2493. https://doi.org/10.1162/jocn_a_01771
Fang, F., & He, S. (2005). Viewer-centered object representation in the human visual system revealed by viewpoint aftereffects. *Neuron, 45*, 793–800.
Finlayson, N. J., Zhang, X., & Golomb, J. D. (2017). Differential patterns of 2D location versus depth decoding along the visual hierarchy. *NeuroImage, 147*, 507–516. https://doi.org/10.1016/j.neuroimage.2016.12.039
Forlim, C. G., Bittner, L., Mostajeran, F., Steinicke, F., Gallinat, J., & Kühn, S. (2019). Stereoscopic rendering via goggles elicits higher functional connectivity during virtual reality gaming. *Frontiers in Human Neuroscience, 13*, 365.
Freud, E., Macdonald, S. N., Chen, J., Quinlan, D. J., Goodale, M. A., & Culham, J. C. (2018). Getting a grip on reality: Grasping movements directed to real objects and images rely on dissociable neural representations. *Cortex, 98*, 34–48. https://doi.org/10.1016/j.cortex.2017.02.020
Gaebler, M., Biessmann, F., Lamke, J.-P., Müller, K.-R., Walter, H., & Hetzer, S. (2014). Stereoscopic depth increases intersubject correlations of brain networks. *NeuroImage, 100*, 427–434. https://doi.org/10.1016/j.neuroimage.2014.06.008
Gerhard, T. M., Culham, J. C., & Schwarzer, G. (2016). Distinct visual processing of real objects and pictures of those objects in 7-to 9-month-old infants. *Frontiers in Psychology, 7*, 827.
Gomez, M. A., Skiba, R. M., & Snow, J. C. (2018). Graspable objects grab attention more than images do. *Psychological Science, 29*(2), 206–218.
Grill-Spector, K., Henson, R., & Martin, A. (2006). Repetition and the brain: Neural models of stimulus-specific effects. *Trends in Cognitive Sciences, 10*(1), 14–23. https://doi.org/10.1016/j.tics.2005.11.006
Grill-Spector, K., & Malach, R. (2001). fMR-adaptation: A tool for studying the functional properties of human cortical neurons. *Acta Psychologica, 107*(1–3), 293–321. https://doi.org/10.1016/S0001-6918(01)00019-1
Hammond, P., & Andrews, D. (1978). Orientation tuning of cells in areas 17 and 18 of the cat's visual cortex. *Experimental Brain Research, 31*(3), 341–351.
Harman, K. L., Humphrey, G. K., & Goodale, M. A. (1999). Active manual control of object views facilitates visual recognition. *Current Biology, 9*(22), 1315–1318.
Harrison, M. T., & Strother, L. (2018). Visual recognition of mirrored letters and the right hemisphere advantage for mirror-invariant object recognition [journal article]. *Psychonomic Bulletin & Review, 25*(4), 1494–1499. https://doi.org/10.3758/s13423-018-1472-3
Heggelund, P., & Albus, K. (1978). Orientation selectivity of single cells in striate cortex of cat: The shape of orientation tuning curves. *Vision Research, 18*(8), 1067–1071.
Holler, D. E., Behrmann, M., & Snow, J. C. (2019). Real-world size coding of solid objects, but not 2-D or 3-D images, in visual agnosia patients with bilateral ventral lesions. *Cortex, 119*, 555–568. https://doi.org/10.1016/j.cortex.2019.02.030
James, T. W., Humphrey, G. K., Gati, J. S., Menon, R. S., & Goodale, M. A. (2002). Differential effects of viewpoint on object-driven activation in dorsal and ventral streams. *Neuron, 35*(4), 793–801. https://doi.org/10.1016/S0896-6273(02)00803-6
Janssen, P., Verhoef, B.-E., & Premereur, E. (2018). Functional interactions between the macaque dorsal and ventral visual pathways during three-dimensional object vision. *Cortex, 98*, 218–227.
Kohn, A., & Movshon, J. A. (2004). Adaptation changes the direction tuning of macaque MT neurons. *Nature Neuroscience, 7*(7), 764–772. https://doi.org/10.1038/nn1267
Konen, C. S., & Kastner, S. (2008). Two hierarchically organized neural systems for object information in human visual cortex. *Nature Neuroscience, 11*(2), 224–231. https://doi.org/10.1038/nn2036
Krekelberg, B., Van Wezel, R. J., & Albright, T. D. (2006). Adaptation in macaque MT reduces perceived speed and improves speed discrimination. *Journal of Neurophysiology, 95*(1), 255–270.
Kriegeskorte, N., Mur, M., & Bandettini, P. A. (2008). Representational similarity analysis-connecting the branches of systems neuroscience. *Frontiers in Systems Neuroscience, 2*, 4.
Logothetis, N. K., & Pauls, J. (1995). Psychophysical and physiological evidence for viewer-centered object representations in the primate. *Cerebral Cortex, 5*(3), 270–288.
Love, J., Selker, R., Marsman, M., Jamil, T., Dropmann, D., Verhagen, J., … Wagenmakers, E.-J. (2019). JASP: Graphical statistical software for common statistical designs. *Journal of Statistical Software, 88*(2), 1–17. https://doi.org/10.18637/jss.v088.i02
Marini, F., Breeding, K. A., & Snow, J. C. (2019). Distinct visuo-motor brain dynamics for real-world objects versus planar images. *NeuroImage, 195*, 232–242. https://doi.org/10.1016/j.neuroimage.2019.02.026
Marr, D., & Nishihara, H. K. (1978). Representation and recognition of the spatial organization of three-dimensional shapes. *Proceedings of the Royal Society of London, Series B: Biological Sciences, 200*(1140), 269–294.
Mordkoff, J. T. (2019). A simple method for removing bias from a popular measure of standardized effect size: Adjusted partial eta squared. *Advances in Methods and Practices in Psychological Science, 2*(3), 228–232. https://doi.org/10.1177/2515245919855053
Nicholls, M. E., Clode, D., Wood, S. J., & Wood, A. G. (1999). Laterality of expression in portraiture: Putting your best cheek forward. *Proceedings of the Biological Sciences, 266*(1428), 1517–1522. https://doi.org/10.1098/rspb.1999.0809
Oliver, Z. J., Cristino, F., Roberts, M. V., Pegna, A. J., & Leek, E. C. (2018). Stereo viewing modulates three-dimensional shape processing during object recognition: A high-density ERP study. *Journal of Experimental Psychology: Human Perception and Performance, 44*(4), 518.
Palmisano, S., Hill, H., & Allison, R. S. (2016). The nature and timing of tele-pseudoscopic experiences. *i-Perception, 7*(1), Article 2041669515625793.
Peissig, J. J., & Tarr, M. J. (2007). Visual object recognition: Do we know more now than we did 20 years ago? *Annual Review of Psychology, 58*, 75–96.
Perrett, D. I., Hietanen, J. K., Oram, M. W., Benson, P. J., & Rolls, E. T. (1992). Organization and functions of cells responsive to faces in the temporal cortex. *Philosophical Transactions of the Royal Society, B: Biological Sciences, 335*, 23–30.
Perrett, D. I., Oram, M. W., Harries, M. H., Bevan, R., Hietanen, J. K., Benson, P. J., & Thomas, S. (1991). Viewer-centered and object-centered coding of heads in the macaque temporal cortex. *Experimental Brain Research, 86*(1), 159–173. . ://WOS:A1991GC83200017.
Perrett, D. I., Smith, P. A., Potter, D. D., Mistlin, A. J., Head, A. S., Milner, A. D., & Jeeves, M. A. (1985). Visual cells in the temporal cortex sensitionve to face view and gaze direction. *Proceedings of the Royal Society of London, Series B: Biological Sciences, 223*, 293–317.
Richardson, J. T. E. (2011). Eta squared and partial eta squared as measures of effect size in educational research. *Educational Research Review, 6*(2), 135–147. https://doi.org/10.1016/j.edurev.2010.12.001
Seriès, P., Latham, P. E., & Pouget, A. (2004). Tuning curve sharpening for orientation selectivity: Coding efficiency and the impact of correlations. *Nature Neuroscience, 7*(10), 1129–1135.
Simons, D. J., Wang, R. F., & Roddenberry, D. (2002). Object recognition is mediated by extraretinal information. *Perception & Psychophysics, 64*, 521–530.
Snow, J. C., & Culham, J. C. (2021). The treachery of images: How realism influences brain and behavior. *Trends in Cognitive Sciences, 25*(6), 506–519.
Snow, J. C., Gomez, M. A., & Compton, M. T. (2023). Human memory for real-world solid objects is not predicted by responses to image displays. *Journal of Experimental Psychology. General*. https://doi.org/10.1037/xge0001387
Snow, J. C., Pettypiece, C. E., McAdam, T. D., McLean, A. D., Stroman, P. W., Goodale, M. A., & Culham, J. C. (2011). Bringing the real world into the fMRI scanner: Repetition effects for pictures versus real objects. *Scientific Reports, 1*, 130. https://doi.org/10.1038/srep00130
Snow, J. C., Skiba, R. M., Coleman, T. L., & Berryhill, M. E. (2014). Real-world objects are more memorable than photographs of objects. *Frontiers in Human Neuroscience, 8*, 837.
Tarr, M. J., & Bülthoff, H. H. (1998). Image-based object recognition in man, monkey and machine. *Cognition, 67*(1–2), 1–20.
Verhoef, B.-E., Vogels, R., & Janssen, P. (2016). Binocular depth processing in the ventral visual pathway. *Philosophical Transactions of the Royal Society, B: Biological Sciences, 371*(1697), Article 20150259.
Wang, X., Baldwin, A. S., & Hess, R. F. (2021). Balanced binocular inputs support superior stereopsis. *Investigative Ophthalmology & Visual Science, 62*(12), 10.
Wang, X. M., & Troje, N. F. (2023). Relating visual and pictorial space: Binocular disparity for distance, motion parallax for direction. *Visual Cognition, 31*(2), 107–125.
Webster, M. A. (2011). Adaptation and visual coding. *Journal of Vision, 11*(5), 3. https://doi.org/10.1167/11.5.3
Weinman, J., & Cooke, V. (1982). Eye dominance and stereopsis. *Perception, 11*(2), 207–210.
Yovel, G., Tambini, A., & Brandman, T. (2008). The asymmetry of the fusiform face area is a stable individual characteristic that underlies the left-visual-field superiority for faces. *Neuropsychologia, 46*(13), 3061–3068.